applied sciences

MDPI

Article

A Numerical Simulation of the Subsidence Reduction Effect of Different Grouting Schemes in Multi-Coal Seam Goafs

Hai Wang [1,2], Yan Qin [1,*], Yuxi Guo [1] and Nengxiong Xu [1]

[1] School of Engineering and Technology, China University of Geosciences (Beijing), Xueyuan Road 29, Beijing 100083, China; wh_rocks@163.com (H.W.); 2102200103@cugb.edu.cn (Y.G.); xunengxiong@cugb.edu.cn (N.X.)
[2] Shanxi Traff Layout Reconnaissance Design Inst., Co., Wuluo St. 27, Taiyuan 030032, China
* Correspondence: qinyancugb@cugb.edu.cn; Tel.: +86-(010)-82322627

Abstract: Grouting is the most widely used technology for treating coal goafs. In this study, a numerical simulation method was used to establish a model of multi-seam goafs with different spacing conditions to investigate the subsidence reduction effects of various grouting schemes on multi-coal seam goafs. By varying the range and opportunity of grouting treatments, the effects of coal seam spacing, grouting treatment range, and grouting opportunity on subsidence reduction were analyzed. The results showed that: (1) With constant overburden (OB), the subsidence reduction ratio of the subgrade center increases linearly as the interburden (IB) decreases ($1 \leq OB/IB \leq 2$), then increases exponentially ($2 < OB/IB$), and eventually becomes stable. (2) When treatment is conducted based on the half-width of the subgrade, the width of the subgrade, and the range of the trapezoid, residual surface subsidence tends to adopt an inclined 'W'-shape in open cutting. The surface residual subsidence exhibits a symmetrical 'W'-shape when full-range grouting is adopted. (3) For a multi-coal seam goaf with longer mining stoppage time, the subsidence reduction ratio of the subgrade center is lower, and it is exponentially related to the grouting opportunity. As the grouting opportunity is extended and OB/IB decreases, the subsidence reduction ratio of the subgrade center declines exponentially.

Keywords: multi-coal seam goaf; range of grouting; opportunity of grouting; subsidence reduction effect; numerical simulation

check for updates

Citation: Wang, H.; Qin, Y.; Guo, Y.; Xu, N. A Numerical Simulation of the Subsidence Reduction Effect of Different Grouting Schemes in Multi-Coal Seam Goafs. *Appl. Sci.* **2023**, *13*, 5522. https://doi.org/10.3390/app13095522

Academic Editor: Bing Bai

Received: 9 April 2023
Revised: 26 April 2023
Accepted: 27 April 2023
Published: 28 April 2023

Copyright: © 2023 by the authors. Licensee MDPI, Basel, Switzerland. This article is an open access article distributed under the terms and conditions of the Creative Commons Attribution (CC BY) license (https://creativecommons.org/licenses/by/4.0/).

1. Introduction

The subsidence area of coal mining in China has exceeded 8000 km^2 and is still growing at a rate of 200 km^2 per year [1–3]. Full-pressure grouting filling, which is an important engineering method, can effectively strengthen the broken rock structure of goafs and reduce the occurrence of deformation disasters in goafs [4–11], and it is widely used in goaf treatment engineering [12–20]. Many experts and scholars have studied the grouting treatment of goafs from the aspects of slurry diffusion, slurry stone strength, and grouting scheme design and have achieved rich research results.

The grouting slurry flows and diffuses under pressure, filling the gaps between broken rock masses. Wang et al. [1] revised a theoretical formula for slurry diffusion based on the distribution characteristics of fractures in a goaf and fracture zones of a single coal seam, as well as the effect of the superposition of porous grouting and the viscosity and diffusion path of the slurry. Yuan et al. [21] independently designed a visual simulation system for grouting in a single coal seam goaf and used it to study the pressure distribution, diffusion radius, and thickness of the stone body of the slurry in the rock layer. The slurry flow showed an approximately elliptical diffusion range under pressure, and the degree of grouting reinforcement increased with distance from the injection borehole, providing a basis for the optimization of the design of grouting in a single coal seam goaf. Yu et al. [22], who took the engineering of a single coal seam goaf roof in weakly cemented siltstone, was

taken as the research background. Methods of field investigation, laboratory testing, and theoretical analysis were adopted. Based on a detailed study of the diffusion of grouting materials, a combined support scheme based on grouting reinforcement and the use of anchor cables was proposed and applied in practical projects. When the slurry diffuses to the designated area for goaf treatment, grouting stones form in the cavities and in areas of the goaf under pressure. The strength of the grouting stones is an important indicator used to measure the effectiveness of grouting reinforcement. Liu et al. [23] conducted grouting tests on the fractured surface of the caving rock mass to solve engineering problems such as rock mass caving in a single coal seam goaf and studied the tensile characteristics of the goaf rock mass after grouting reinforcement. Xie et al. [24] applied numerical simulations to analyze the effective pre-stress field distribution of broken roof and grouting roof anchor cables in a multi-seam goaf. The strength of grouting stone bodies in a multi-coal seam goaf was monitored using experimental laboratory methods, and a treatment method of using grouting anchor cables to fix the weak surface of the roof plate and seal roof cracks was proposed. Han et al. [25] revealed the stress-hardening characteristics and load-bearing mechanism of grouting stones in uniaxial compression tests by conducting experiments on their physical properties. Modoni et al. [26] proposed a method for predicting the strength of grouted stone bodies based on their interaction with surrounding rock and soil. Zong et al. [27] conducted uniaxial compression tests on fractured rock masses after grouting and found the influences of grouting stone strength, deformation characteristics, and failure mode on the grouting reinforcement effect. They also found that the failure mode of the sample changed from brittle failure to plastic failure. The above research results provide a basis for grouting treatment technology, and experts and scholars have conducted research on the effect of grouting treatment plans on subsidence reduction. Wang et al. [28] combined numerical simulation and laboratory experiments and proposed a grouting method for preventing and controlling safety hazards in a single coal seam goaf by using pre-drilling, full-hole intubation, extended sealing, and multi-stage drilling for grouting. Li et al. [19] used numerical simulation software to simulate the reinforcement effects of two grouting methods—full-range grouting and strip grouting—in a single coal seam goaf. They found that a reasonable grouting plan can effectively reduce residual deformation of the goaf and its overlying rock mass, improve adverse stress conditions, and achieve the goal of effective grouting. Based on a theory of mining subsidence, Deng et al. [29] studied grouting filling technology to control the residual subsidence of a single coal seam goaf and concluded that under a certain mining depth, goaf grouting can be filled with banded grouting. The grouting hole should be arranged within 20 m of the edge of the working face, in the direction of the steeply inclined coal seam and the fault development area to fill the voids and under-compacted areas at the edge of the goaf. To explore the grouting scheme of multi-coal seam goafs, Chen et al. [30] studied the grouting treatment technology of multi-coal seam goafs by combining various geophysical exploration methods and drilling methods. According to the spacing of each coal seam goaf, the grouting horizon was divided, and the grouting technology and scheme of "pressure less gravity flow and pressurized diffusion" were used to reinforce the goaf. He et al. [31] used methods such as on-site investigation, laboratory testing, and numerical simulation to study the deformation and failure modes and stress distribution characteristics of multi-seam goafs at close range under double-thick coal seam mining conditions. A zoning grouting treatment method centered on "high pressure water jet, asymmetric high strength cable beam net, three hole anchor cable group and roof grouting" was proposed.

Most of the above studies focused on the treatment of single-coal seam grouting. Due to the large burial depth and multiple layers of goaf in multi-coal seam goafs, if grouting is carried out according to the recommended standard [32] and the grouting range is determined based on the rock movement angle, then it causes the grouting range to be too large, which affects the ecological protection and restoration of the grouting area and may not necessarily achieve the expected subsidence reduction effect. The selection of grouting treatment opportunity also directly affects the residual subsidence level of multi-seam goafs.

The goal of this study was to further clarify the control of the effects of different grouting schemes on the deformation of multi-coal seam goafs. A model of a multi-coal seam goaf with different spacing conditions was designed using a numerical simulation method. By changing the grouting range and opportunity, the long-term deformation of multi-coal seam goafs with different spacings after different grouting schemes was calculated, and the subsidence reduction effect of different grouting schemes on the deformation of multi-coal seam goafs was analyzed. The results can provide more scientific and reliable guidance for the treatment of multi-seam goafs.

2. Proposed Method

This study establishes a numerical model of multi-coal seam goafs with different spacing, selects an appropriate constitutive model, considers different grouting treatment ranges and opportunities in the multi-coal seam goaf grouting treatment plan, studies the grouting subsidence reduction effect of different grouting schemes on multi-coal seam goafs, and reveals the influences of grouting opportunity and range selection on the treatment of multi-coal seam goafs.

2.1. Establishment of a Numerical Model of a Multi-Seam Goaf

Previous studies have shown that FLAC calculation software can effectively simulate coal seam mining and grouting treatment problems [33,34]. The Moh–Coulomb model, a double-yield model, and Burgers' model can effectively simulate coal seam mining, grouting treatment, and long-term deformation of goaf. The numerical model of the multi-coal seam goaf was a pseudo-3D model with a thickness of 4 m for both the upper and lower coal seams, and the overlying rock lithology was medium-hard rock. According to the standard [33], the thickness of the caving zone was calculated to be 10 m. To ensure sufficient mining, the lengths of the upper and lower coal seam working faces were taken as 1000 m. In each working condition, the thickness of the overburden above the upper coal seam was taken as 100 m, and the thickness of the bottom plate below the lower coal seam was taken as 40 m, as shown in Figure 1.

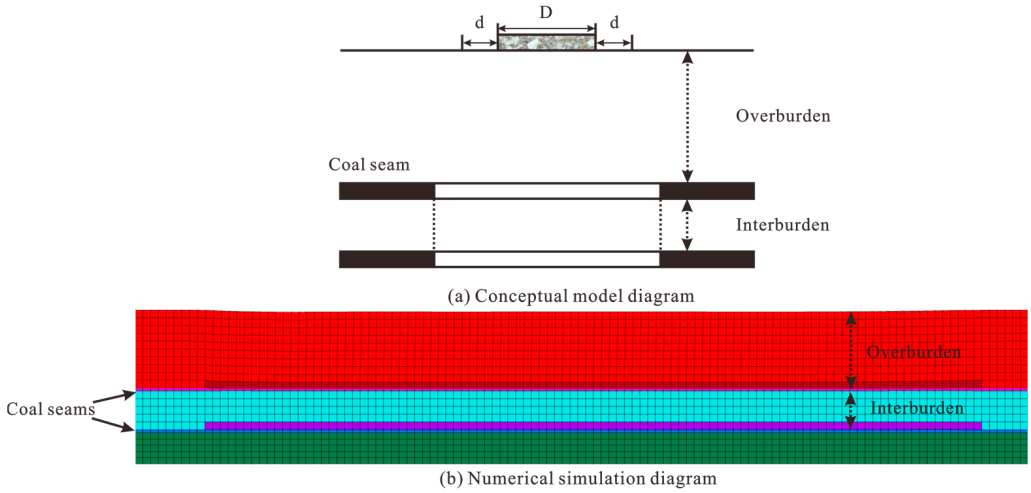

Figure 1. Completely overlapping mining schematic diagram.

Ten sets of multi-coal seam goaf spacing models were designed, all of which used the same overburden (OB) and different the interburden (IB). The dimensions of the upper and lower coal seam working faces were the same, but the burial depth in the longitudinal direction differed. The spacing information of the coal seams is shown in Table 1.

Table 1. Design table for spacing of multi-coal seam goaf.

Case Number	Overburden (OB)/m	Interburden (IB)/m	Working Face Length
1	100	10	1000 m for both upper and lower coal seam working faces
2		20	
3		30	
4		40	
5		50	
6		60	
7		70	
8		80	
9		90	
10		100	

This model adopted hexahedral mesh generation with a mesh size of 10 m. The displacement in the x-direction of the left and right boundaries of the model, the displacement in the y-direction of the front and rear boundaries, and the displacement in the z-direction of the lower boundary were fixed. The upper boundary was a free boundary. In the calculation, the self-weight of the rock mass was considered, the value of acceleration due to gravity in the model was 9.80 m/s^2, and the mining step distance was 10 m.

(1) Calculation models

For unexcavated coal seams and surrounding rocks, the Mohr–Coulomb model is used for calculation. During the equivalent mining process, a double-yield model is used to simulate the compaction process of collapsed rock masses in the caving zone. After the mining is completed, Burgers' model is used to dynamically assign creep parameters to the units within the corresponding interval range to calculate the creep process of the collapsed rock mass in the caving zone.

(2) Calculation parameters

To prevent the impact of different lithological combinations on the calculation results, the calculation parameters for the surrounding rock in this study were unified as medium-hard rock calculation parameters. Based on relevant laboratory experiments and engineering experience, the engineering analogy method was used to determine the calculation parameters for each layer in this study, as shown in Table 2. The equivalent mining method was used to assign the mined coal seam and the rock mass in the caving zone to a double-yield model to simulate the compaction process of the fractured rock mass. The calculation parameters are shown in Table 3 [33]. After mining in the goaf is stopped, the fractured rock mass and grouting stone mass undergo creep deformation under the pressure of the overlying rock layer. Burgers' model must be assigned to the designated area, and the calculation parameters are shown in Tables 4 and 5 [34].

Table 2. Calculation parameters for each layer.

Stratum	ρ (kg/m^3)	E_T (GPa)	ν	c (MPa)	φ (°)	σ_t (MPa)
Overlying rock	2750	3.20	0.25	1.00	30	0.35
Coal	1380	0.45	0.34	0.17	20	0.05
Floor	2750	3.20	0.25	1.00	30	0.35

Table 3. Calculation parameters of the double-yield model [33].

ρ (kg/m^3)	Maximum Bulk Modulus (GPa)	Maximum Shear Modulus (GPa)	c (MPa)	φ (°)	Plastic Modulus Multiplier
1680	2.24	1.41	0	15	3.0

Table 4. Calculations of creep parameters of medium-hard rock [34].

Creep Parameters	Compressive Stress Range/MPa	Parameter Calculation Formula
K/MPa	$0 < \sigma_{zz}$	$K = 6.35\ \sigma_{zz}^{1.78}$
G_m/MPa	$0 < \sigma_{zz} < 6.16$	$G_m = -6.82\ \sigma_{zz} + 344$
	$6.16 < \sigma_{zz} < 9.24$	$G_m = 2.92\ \sigma_{zz} + 284$
	$9.24 < \sigma_{zz}$	$G_m = -747\ \sigma_{zz} + 380$
G_k/MPa	$0 < \sigma_{zz}$	$G_k = 27.27\ \sigma_{zz} - 59$
η_m/MPa·h	$0 < \sigma_{zz} < 6.16$	$\eta_m = 11{,}613.96\ \sigma_{zz} + 11{,}446$
	$6.16 < \sigma_{zz} < 9.24$	$\eta_m = -5721.46\ \sigma_{zz} + 118{,}232$
	$9.24 < \sigma_{zz}$	$\eta_m = -850.812\ \sigma_{zz} + 73{,}227.5$
η_k/MPa·h	$0 < \sigma_{zz} < 6.16$	$\eta_k = -26.62\ \sigma_{zz} + 4728$
	$6.16 < \sigma_{zz} < 9.24$	$\eta_k = 55.19\ \sigma_{zz} + 4224$
	$9.24 < \sigma_{zz}$	$\eta_k = -42.86\ \sigma_{zz} + 4338$

Table 5. Calculations of creep parameters of grouting stone [34].

Creep Parameters	Parameter Calculation Formula
K/MPa	$K = 5.18697 \times e^{\frac{\sigma 1}{3.75492}} + 31.74$
G_m/MPa	$G_m = 40.4643 \times \sigma_1 + 41.5749$
G_k/MPa	$G_k = -1111.16204 + 776.47378 \times \sigma_1 - 81.25659 \times {\sigma_1}^2 + 2.97386 \times {\sigma_1}^3 \times 10^{-2}$
V_m/MPa·h	$V_m = 9 \times 10^9$
V_k/MPa·h	$V_k = 17088.0167 - 9300.51676 \times \sigma_1 + 1337.43539 \times {\sigma_1}^2$

2.2. Design of Different Grouting Ranges

Figure 2 shows a schematic diagram of the treatment range of the goaf in a horizontal multi-coal seam goaf. In this simulation plan, four types of grouting treatment ranges are designed:

(1) Treatment within the half-width of the subgrade. As shown in the blue line area in Figure 2, the treatment width of the goaf caving zone in both the upper and lower coal seams was 40 m.
(2) Treatment within the width of the subgrade. As shown in the green line area in Figure 2, the treatment width of the goaf caving zone in both the upper and lower coal seams was 80 m.
(3) The standard suggests the treatment of the trapezoidal range [32]. This treatment is as shown in the red line area in Figure 2 below.
(4) Full-range treatment of the working face. As shown in the black line area in Figure 2, grouting treatment was carried out throughout the goaf caving zone of the upper and lower coal seams, with a treatment width of 1000 m.

This numerical simulation studies the impact of different grouting treatment ranges on the control and effect of subsidence reduction in multi-seam goafs by changing the grouting width within the range of the caving zone in the multi-seam goaf. Taking the grouting treatment condition with a spacing of 10 m between the upper and lower coal seams as an example, the design schemes for different grouting treatment ranges are shown in Table 6.

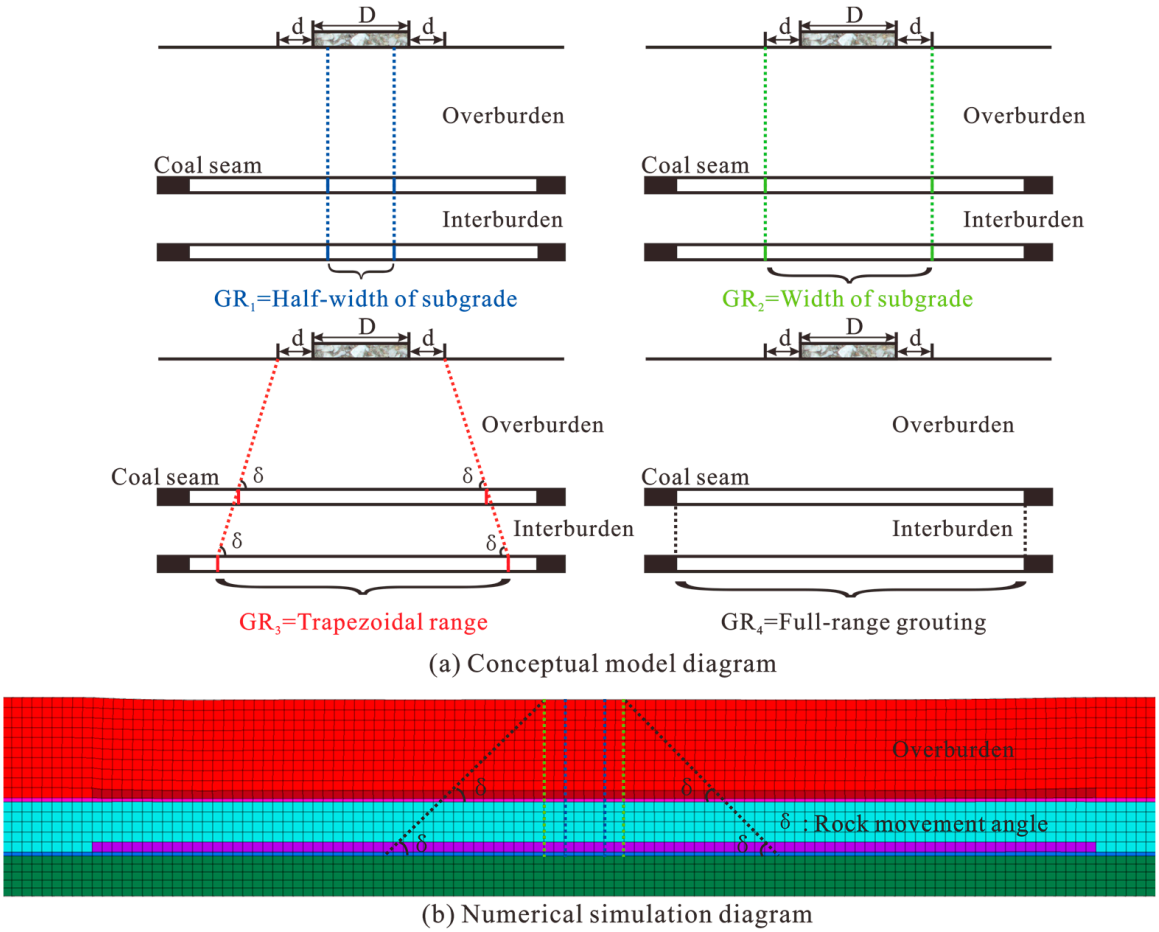

Figure 2. Diagram of the multi-seam goaf grouting ranges.

Table 6. Design of different grouting treatment ranges.

Interburden/m	Grouting Opportunity	Grouting Ranges (GR)
IB = 10	Immediate grouting	GR_1 = Half-width of subgrade GR_2 = Width of subgrade GR_3 = Trapezoidal range GR_4 = Full-range grouting

2.3. Design of Different Grouting Opportunity Schemes

This study uses numerical simulation to study the effect of grouting opportunity on the subsidence reduction effect of multi-seam goaf grouting. Taking the full-range grouting treatment condition with a spacing of 50 m between the upper and lower coal seams as an example, the design of different grouting opportunity schemes is shown in Table 7.

Table 7. Design of different grouting opportunities.

Interburden/m	Grouting Ranges	Grouting Opportunity (Time Interval between Stopping Mining)/Year
IB = 50	GR_4	GO_1 = 0.0 GO_2 = 0.5 GO_3 = 1.0 GO_4 = 1.0 GO_5 = 2.0 GO_6 = 2.5 GO_7 = 3.0

First, the upper coal seam working face is excavated, and then Burgers' model is applied to the rock mass in the caving zone to calculate the long-term deformation within one year. Then, the working face of the lower coal seam is excavated, and different grouting opportunities are selected to carry out comprehensive grouting treatment on the goaf of the upper and lower coal seams. Finally, the long-term deformation of the surface after 10 years is calculated, and the subsidence pattern of the subgrade center is recorded. From this, it is possible to simulate the subsidence of the subgrade center and the amount of grouting reduction when grouting is carried out in the goaf at different points in time after the completion of multi-coal seam mining and to obtain the impact of grouting opportunity on the grouting reduction effect in the goaf of multi-coal seams.

3. Results and Discussion

3.1. Results of Calculations of Grouting Subsidence Reduction in Goaf Areas with Different Spacing

Based on the method described earlier, the residual subsidence of the surface after grouting was simulated under different coal seam spacing conditions. The calculation results are shown in Figure 3, which are the residual subsidence cloud maps of grouting with coal seam spacings of 10 m, 30 m, 50 m, 70 m, and 90 m. From the residual subsidence cloud maps of grouting, it can be concluded that under different coal seam spacing conditions, after grouting treatment, the residual subsidence value of the surface near the stop mining line and the opening hole is relatively large. In contrast, the residual subsidence value of the surface near the center of the roadbed is relatively small, and as the burial depth of goaf in multi-coal seam increases, the residual subsidence after surface grouting treatment gradually increases. When the distance between coal seams reaches 70 m, there is little difference in the residual subsidence cloud maps of multi-coal seam goaf, and the influence of coal seam distance on the grouting treatment effect of multi-coal seam goaf is weakened. The cantilever beam structure of the roof near the opening and stopping lines in the goaf of the multi-coal seam is relatively long, resulting in under-compaction in this area. Therefore, there will still be some subsidence after grouting treatment compared to the compacted area below the surface subsidence basin. The greater the burial depth of the goaf in the multi-coal seam, the greater the pressure on the goaf from the overburden, resulting in more significant residual subsidence after treatment [22].

According to the calculation results in Figure 3, the subsidence of the subgrade center under grouted and non-grouted conditions for the spacing conditions of each coal seam are calculated and recorded as L_1 and L_2, respectively. Then, the grouting subsidence reduction for different coal seam spacing conditions is calculated according to Equation (1) for ΔL. According to Equation (2), the grouting subsidence reduction rate R is obtained for different coal seam spacing conditions.

$$\Delta L = L_1 - L_2 \tag{1}$$

$$R = \Delta L / L_1 \tag{2}$$

The relationship between the center subsidence reduction ratio R of the subgrade and the distance between coal seams is shown in Figure 4. From the figure, it can be concluded that when the spacing between coal seams is 10 m, the grouting has the best effect on reducing subsidence, and the ratio of subsidence reduction at the center of the subgrade can reach 81.1%. As the spacing between coal seams continues to increase, the ratio of subsidence reduction at the center of the subgrade gradually decreases after grouting treatment. When the spacing between coal seams is greater than 80 m, the rate of decrease in the center subsidence rate of the subgrade gradually decreases with the increase in the spacing between coal seams, and the curve tends to be flat. During the process of increasing the spacing between coal seams from 10 m to 80 m, the reduction ratio significantly decreases from 81.1% to 50.1%. Afterwards, the reduction ratio at the center of the subgrade is approximately 46%, and there is no significant change with the increase in the spacing between coal seams.

Residual subsidence time : 10 years ;

Selection of grouting scheme:

①Coal seam spacing selection scheme IB=10、30、50、70、90m ;

②Grouting treatment range selection scheme GR_4 ;

③Grouting opportunity selection scheme GO=0year ;

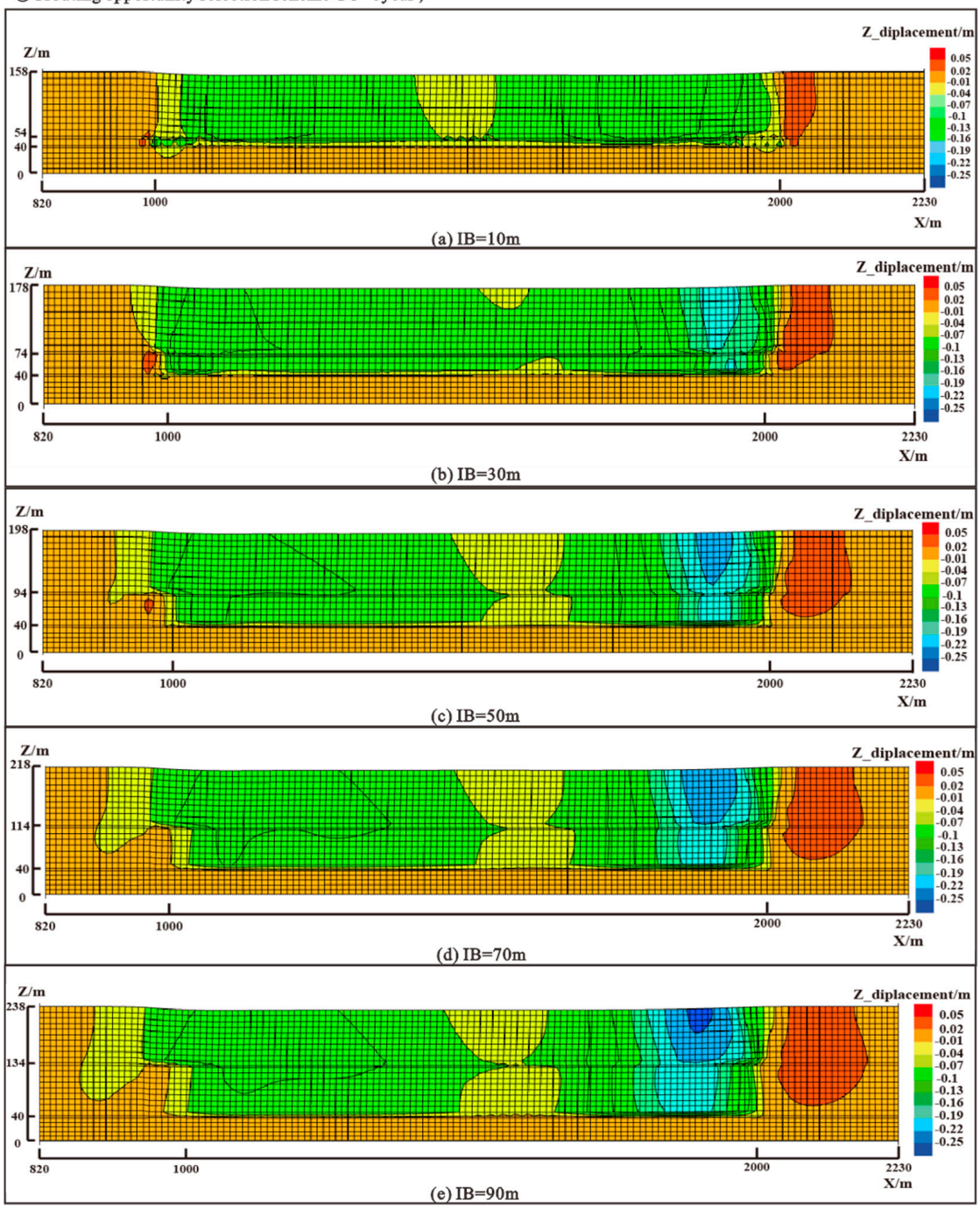

Figure 3. Grouting residual subsidence nephogram of different coal seam spacings.

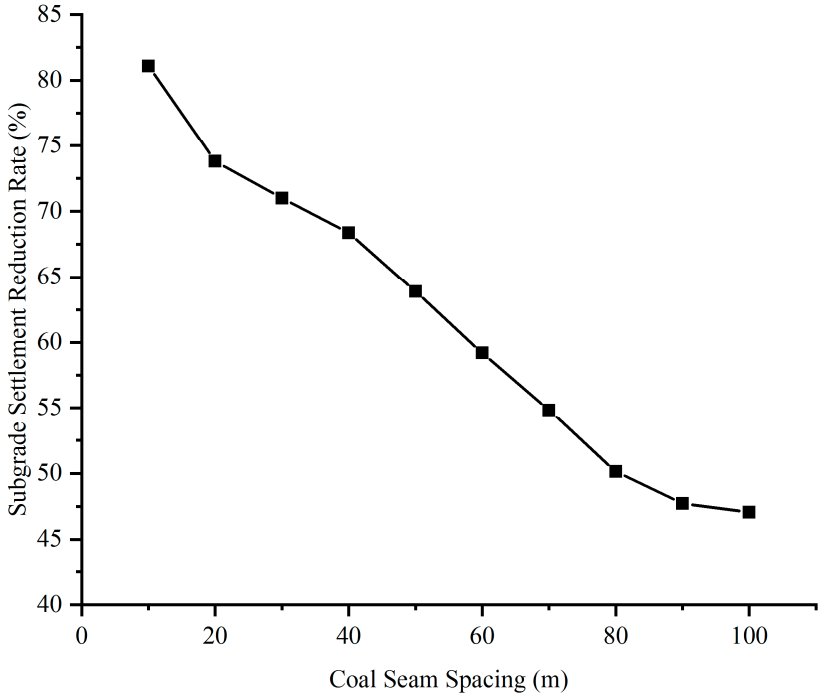

Figure 4. The subsidence reduction rate for subgrade center grouting treatment under different spacing conditions.

Figure 5 shows the relationship between the center subsidence reduction rate of the subgrade and OB/IB after grouting treatment with different coal seam spacing. From the graph, it can be concluded that when the burial depth (OB) of the upper coal seam is constant, the ratio of subgrade center subsidence reduction after grouting treatment first increases linearly ($1 \leq$ OB/IB ≤ 2), then increases exponentially ($2 <$ OB/IB), and finally tends to be flat.

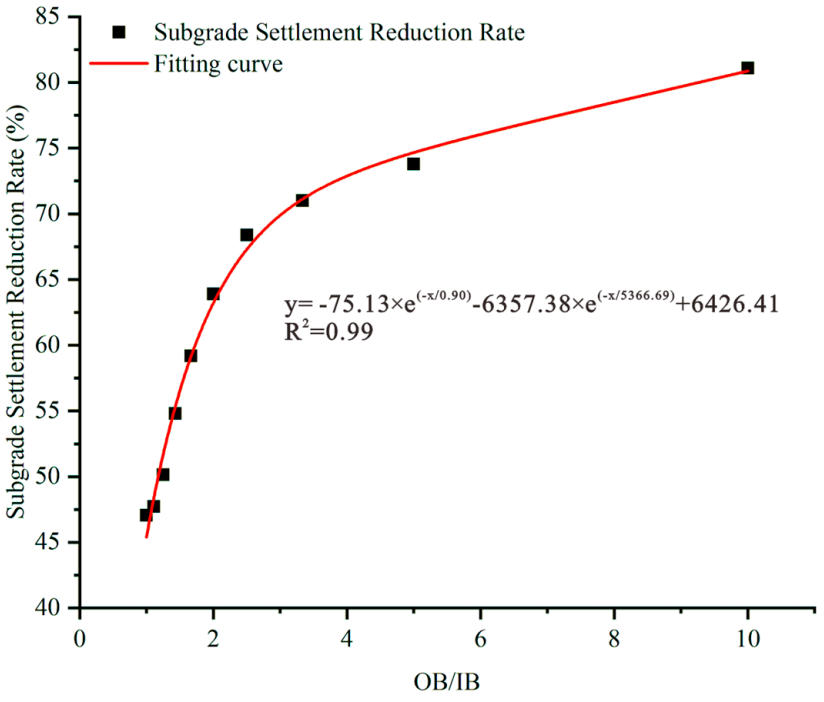

Figure 5. The subsidence reduction rate of subgrade center grouting treatment for different OB/IB conditions.

In summary, due to the large spacing between coal seams, the OB/IB is relatively small. At this time, the compaction amount of the lower coal seam caving zone is relatively large, and the upper coal seam caving zone and crack zone undergo compaction and closure under the disturbance, resulting in poor grouting treatment and a subsidence reduction effect. When the spacing between coal seams is small and OB/IB is larger, the load on the overlying rock mass is smaller, and the long-term deformation of the reinforcement after grouting is reduced, making the grouting subsidence reduction effect better.

3.2. Calculation Results of Subsidence Reduction in Goaf Areas of Multi-Coal Seam Goafs with Different Grouting Ranges

To analyze the impact of different grouting treatment ranges on the subsidence reduction effect of grouting in multi-coal seam goafs, this study considered four grouting treatment ranges: half-width range of subgrade, width range of subgrade, trapezoidal range, and full-range grouting. Figure 6 shows the residual subsidence cloud map of the goaf under different grouting treatment conditions. From the residual subsidence cloud maps of grouting, it can be concluded that under different grouting range conditions, the residual subsidence near the goaf opening and stopping line is relatively more significant than that in the mining center area. When grouting is carried out in the goaf of multi-coal seam according to the half-width of the subgrade, the width of the subgrade, and the trapezoidal range, the residual subsidence at the subgrade is controlled, and the overall residual subsidence control effect of the model after full-range grouting is the most obvious. This is because when grouting is carried out according to the width of the subgrade, half-width of the subgrade, and the trapezoidal range, the broken rock masses near the stop mining line are not treated, resulting in damage to the cantilever beam structure near the stop mining line when residual subsidence occurs, and large-scale subsidence occurs at the stop mining line. According to the full range of grouting, the damage of the cantilever beam structure near the stop mining line is controlled, forming a relatively stable structure, and the most obvious effect of reducing subsidence control is achieved [30].

Figure 7 shows the surface residual subsidence curve for different grouting treatment scopes. The results show that when using full-range grouting treatment, the residual subsidence on the surface presents a symmetrical "W"-shape on both sides. The overall trend of the fluctuations of the residual subsidence curve in the "W"-shape is relatively stable, and the best subsidence reduction effect is achieved. When grouting treatment is performed according to the entire width of the subgrade, half-width of the subgrade, and trapezoidal range, this results in damage to the cantilever beam structure near the stopping line during residual subsidence. The residual subsidence shows a tilted "W"-shape inclined toward the opening.

Figure 8 shows the amount of subsidence reduction ΔL and the ratio of R at the center of the subgrade for the range of grouting treatments. From the figure, it can be concluded that when using the full-range grouting treatment, the grouting has the best effect on reducing subsidence. At this time, the subsidence reduction amount and ratio at the center of the subgrade are 0.158 m and 81.1%, respectively. When the grouting treatment range is trapezoidal, the width of the subgrade, or half-width of the subgrade, the subsidence reduction rate at the center of the subgrade gradually decreases. Therefore, during the same period after the completion of mining, the maximum controlled residual subsidence value of the surface can be achieved when the treatment width is the full-range of the caving zone, followed by the trapezoidal range > the width of the subgrade > the half-width of the subgrade.

The inclination value and uneven subsidence control rate caused by uneven subsidence of the subgrade for different grouting treatment ranges are plotted in Figure 9. From the figure, it can be concluded that when the treatment width is selected within the range of subgrade width or half-width of the subgrade, the improvement effect on uneven subsidence of the subgrade is poor. When the treatment width is selected as trapezoidal and full-range grouting, the uneven subsidence of the subgrade is significantly improved.

After mining, the goaf is immediately treated with full-range grouting, with a control rate of over 95% for uneven subsidence of the subgrade. Trapezoidal range grouting is used with a control rate of over 56% for uneven subsidence of the subgrade.

Residual subsidence time : 10 years ;

Selection of grouting scheme:

①Coal seam spacing selection scheme IB=10m ;

②Grouting treatment range selection scheme GR_1~GR_4 ;

③Grouting opportunity selection scheme GO_1 ;

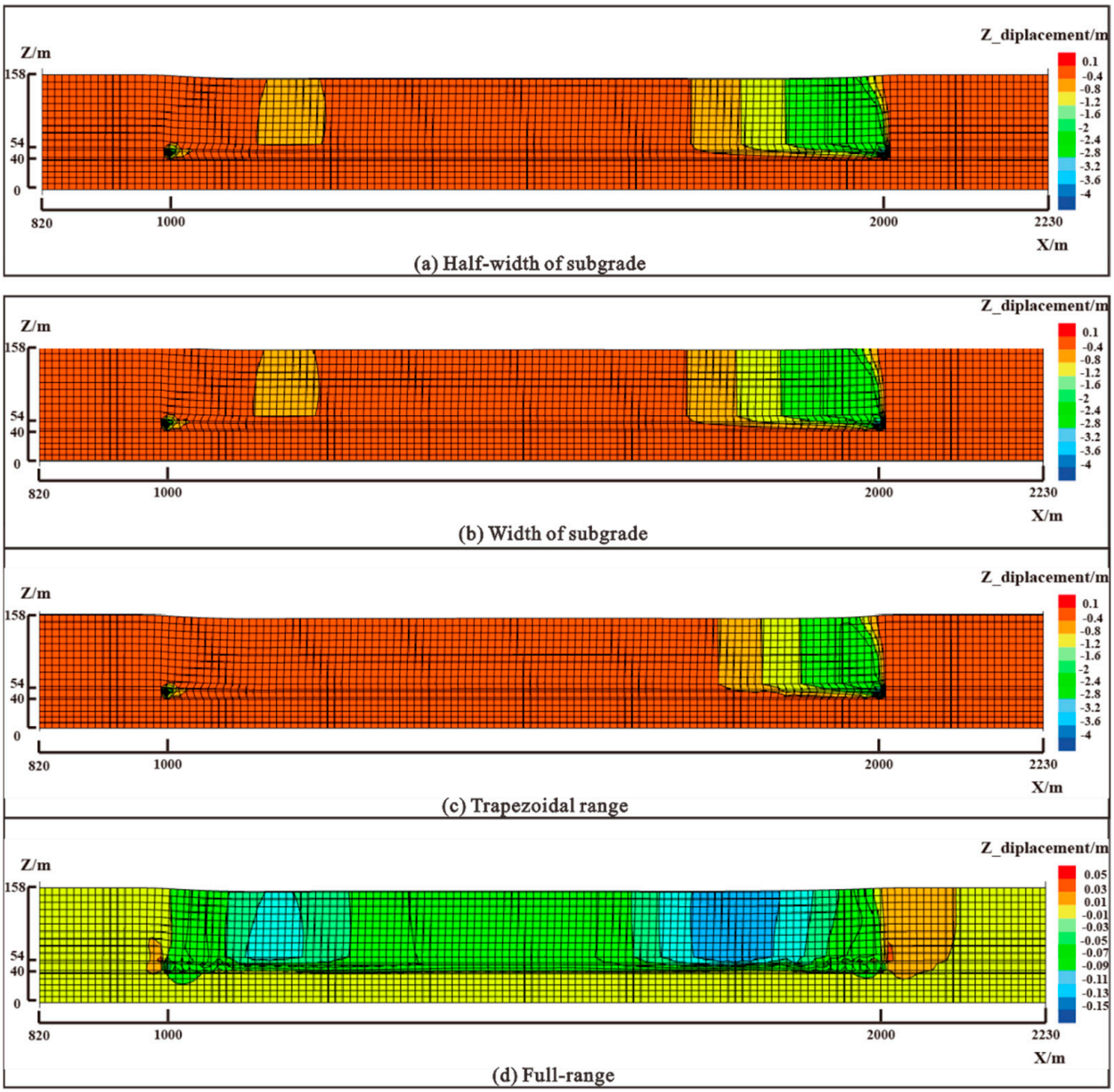

Figure 6. Residual subsidence nephogram for different grouting ranges.

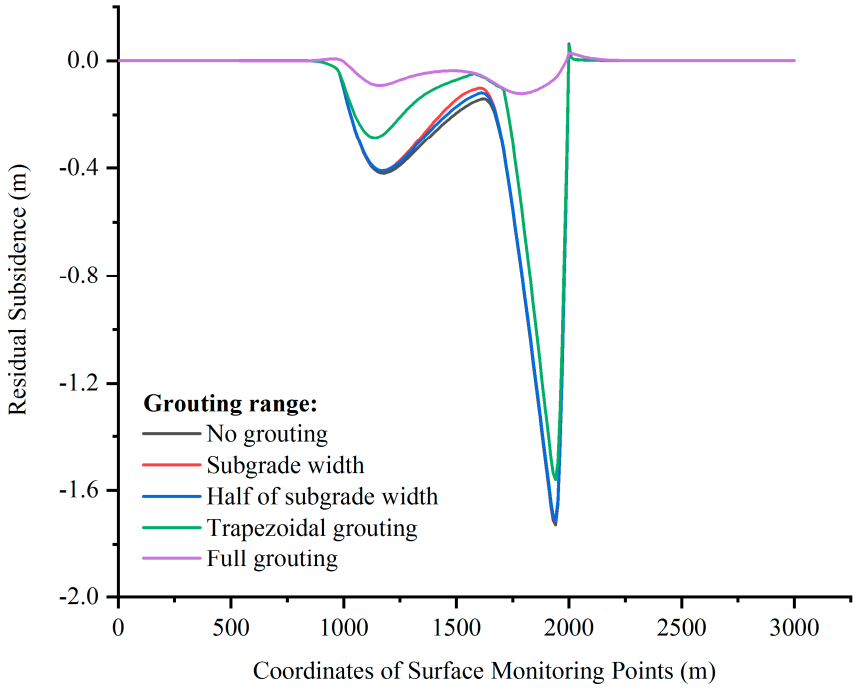

Figure 7. The surface subsidence curve for different grouting range conditions.

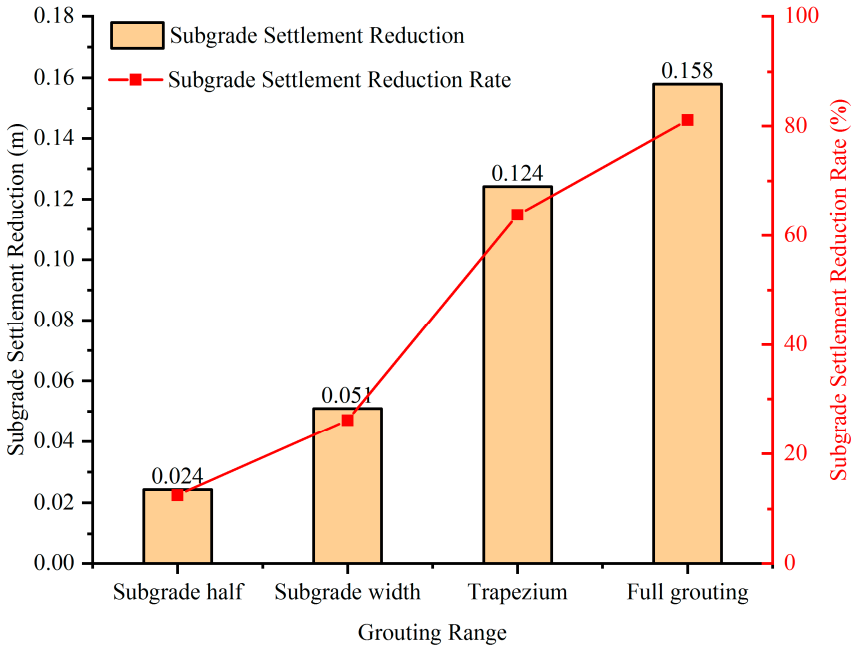

Figure 8. The amount of subsidence reduction and the subsidence reduction rate of the subgrade center for different grouting range conditions.

In summary, when the treatment width adopts the trapezoidal range and full-range grouting, the subsidence reduction at the center of the subgrade and uneven subsidence of the subgrade are significantly improved. Through simulation calculations, when the treatment width is treated according to the trapezoidal range and the control effect meets the standard requirements, the trapezoidal range can be used for treatment. The advantage is that the trapezoidal range has a smaller width than the full-range grouting treatment, and the impact on the environment after grouting treatment is relatively small, which reduces engineering costs and shortens the construction period. If the engineering and regulatory

requirements are not met, then full-range grouting can be used for prevention and control, which can achieve good subsidence control effects.

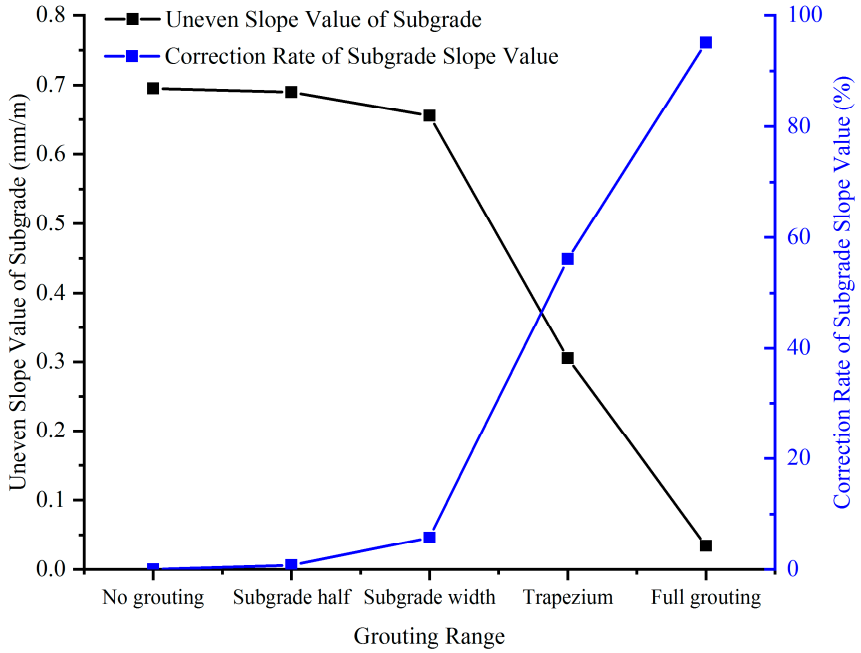

Figure 9. Subgrade incline value and incline reduction rate for different grouting range conditions.

3.3. Results of Calculations of Grouting Subsidence Reduction for Different Grouting Opportunities

This study considers conducting full-range grouting treatment within 0 to 3 years after multi-seam mining. Figure 10 shows the calculation results for the cloud maps of the residual subsidence of the goaf for different grouting opportunity conditions. The residual subsidence contour indicates grouting is carried out closer to the mining stopping on the working face, resulting in more residual subsidence in the goaf of the multi-coal seam, effectively controlling surface subsidence. When grouting is carried out after mining stops for two years, there is little difference in the subsidence contours of the goaf in the multi-coal seam. In addition, the impact of grouting opportunities on the grouting treatment effect of the goaf in the multi-coal seam is weakened, since the residual subsidence capacity of the goaf in the multi-coal seam gradually weakened after the completion of coal seam excavation. Therefore, when the residual subsidence capacity is large, grouting at a time point closer to the cessation of mining can produce better grouting and subsidence reduction effects. In summary, the later the grouting opportunity is, the greater the residual subsidence in the goaf of the multi-coal seam that has already occurred before grouting, resulting in a small amount of grouting subsidence reduction and poor grouting subsidence reduction effect.

The relationship between the subsidence reduction ratio R at the center of the subgrade and the opportunity for grouting is plotted in Figure 11. From the graph, it can be concluded that immediately after the coal seam is mined, grouting has the best effect on reducing subsidence with a subsidence reduction ratio of 67.2% at the center of the subgrade. The longer the distance from stopping mining, the subsidence reduction ratio at the center of the subgrade gradually decreases after grouting treatment, and the subsidence reduction rate curve shows an exponential relationship. When grouting is carried out after mining is stopped for 2 years with the extension of grouting opportunity, the rate of decrease in the center subsidence rate of the subgrade gradually decreases, and the curve tends to be flat.

Residual subsidence time : 10 years ;

Selection of grouting scheme :

① Coal seam spacing selection scheme IB=50m ;

② Grouting treatment range selection scheme GR_4 ;

③ Grouting opportunity selection scheme GO=0、1、2、3 year;

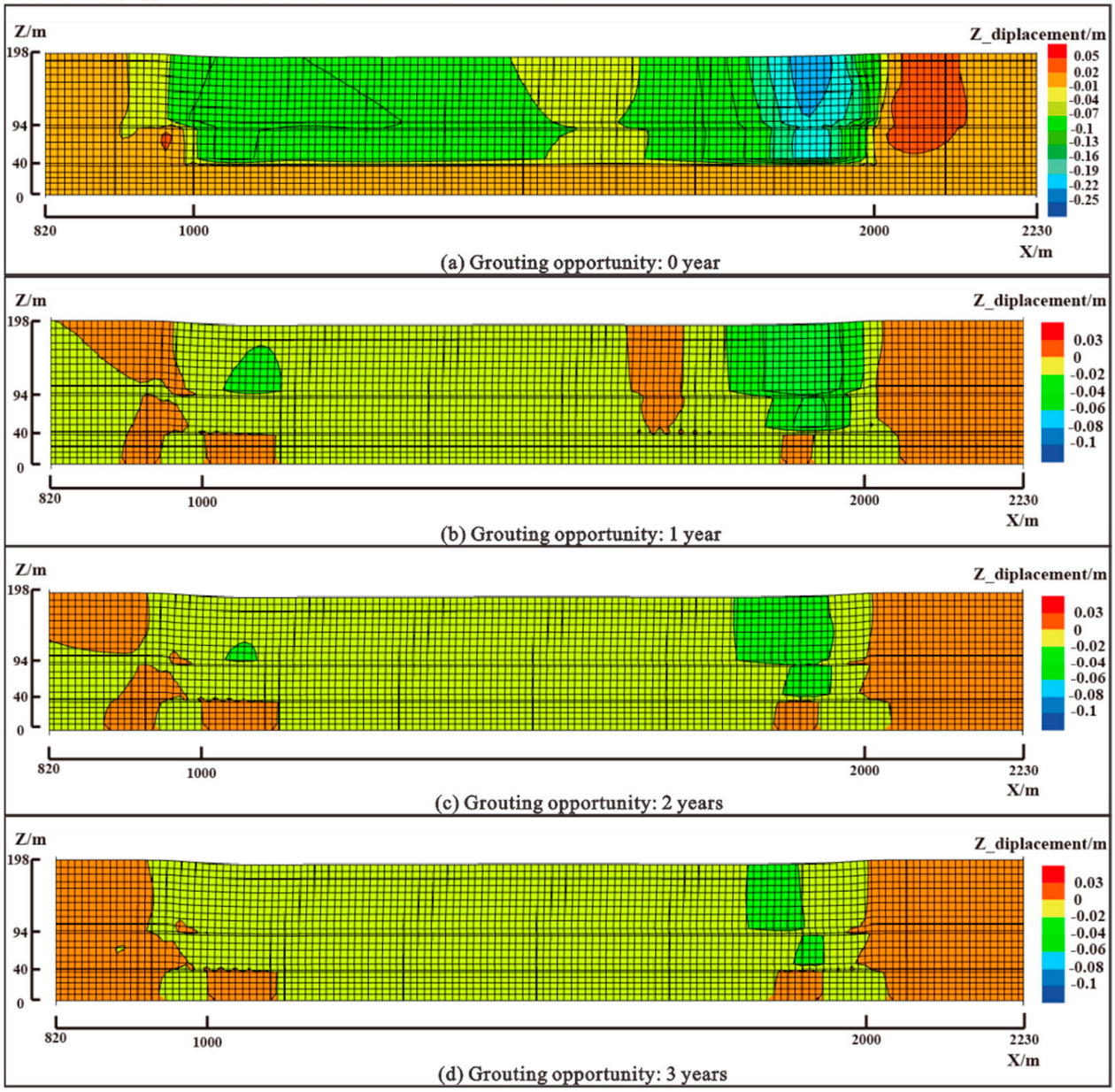

Figure 10. Residual subsidence nephogram for different grouting opportunity conditions.

In summary, due to the completion of the excavation of the working face, the surface subsidence rate gradually slows, and the residual deformation capacity gradually decreases. When the residual deformation capacity is large then grouting is performed closer to the completion of the excavation of the working face, which can produce better grouting and subsidence reduction effects.

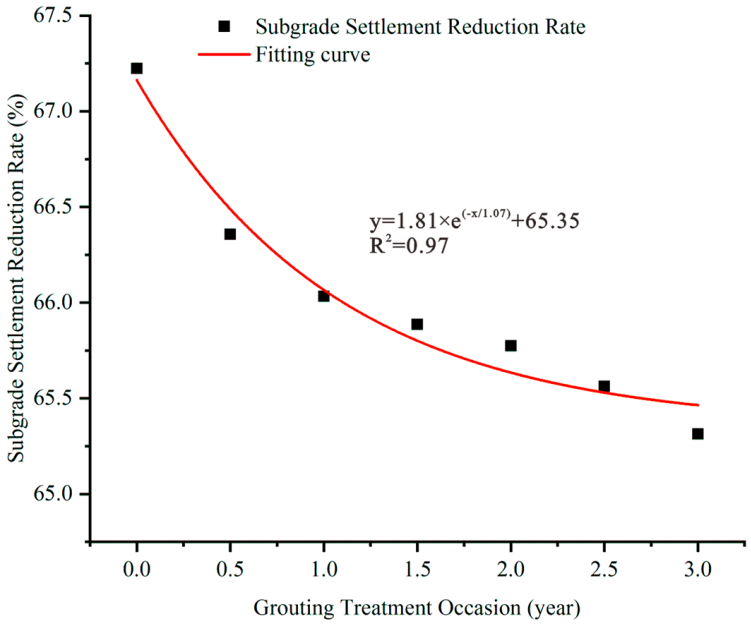

Figure 11. Subgrade center subsidence reduction rate for different grouting opportunity conditions.

Figure 12 shows the variation of the center subsidence reduction ratio of the subgrade for different grouting opportunities and coal seam spacing conditions. From the figure, it can be seen that with the extension of grouting opportunity and the decrease in OB/IB, the subsidence reduction ratio at the center of the subgrade decreases exponentially. When $1 \leq$ OB/IB ≤ 2 and grouting is carried out 2 years after excavation, the subsidence reduction ratio of the subgrade center decreases rapidly, and the grouting treatment effect is poor. This is because increasing the spacing between coal seams can lead to increased deformation of the surface and goaf, and even with grouting treatment, it is difficult to completely prevent the problem of surface subsidence. With the extension of grouting opportunity, there is a significant amount of residual deformation in the goaf, resulting in a decrease in the contact area between grouting materials and fractured rock masses and cracks in the goaf, which influences the grouting effect.

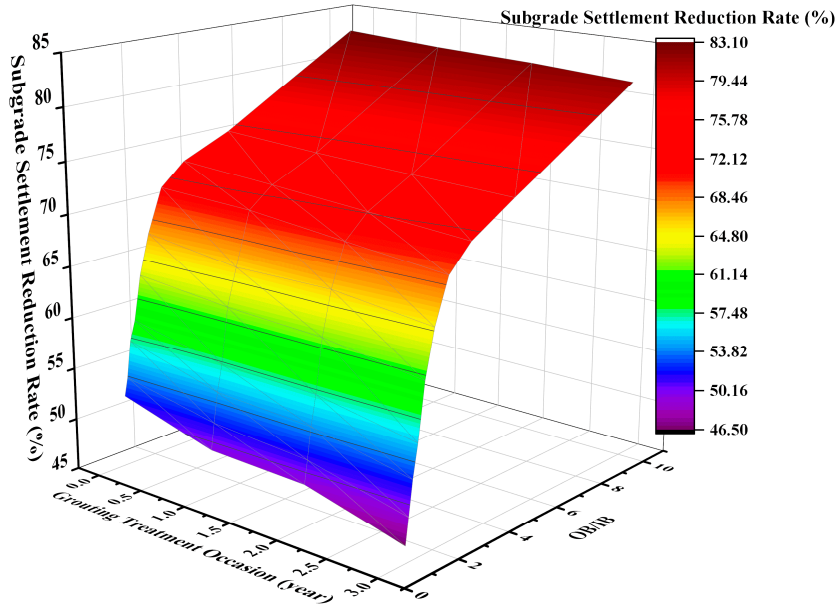

Figure 12. Diagram of the relationship between grouting opportunity, OB/IB, and subgrade center subsidence reduction rate.

4. Conclusions

Currently, there is no dependable foundation for constructing grouting treatment plans for multi-seam goafs. This study adopted a numerical simulation method to design models of multi-coal seam goafs with different spacing conditions. By changing the grouting range and opportunity, the influence of coal seam spacing, grouting range, and grouting opportunity on the subsidence reduction effect of multi-coal seam goafs was studied. The main conclusions are as follows:

(1) With constant overburden (OB), the subsidence reduction ratio of the subgrade center increases linearly as the interburden (IB) decreases ($1 \leq OB/IB \leq 2$), then increases exponentially ($2 < OB/IB$), and eventually becomes stable.

(2) When the treatment is performed according to the half-width of the subgrade, the width of the subgrade and the range of a trapezoid, the surface residual subsidence tends to the inclined 'W'-shape of the open cutting. The surface residual subsidence has a symmetrical 'W'-shape when full-range grouting is adopted. When the treatment width is selected as the width of the subgrade or half-width of the subgrade, the improvement effect on uneven subsidence of the subgrade is poor. When the treatment width is selected as the trapezoidal range and full-range grouting, the uneven subsidence of the subgrade is significantly improved.

(3) For the grouting treatment of goaf areas with multi-coal seam goafs where mining has been stopped for a longer time, the central subsidence reduction rate of the subgrade is smaller, and there is an exponential relationship between the central subsidence reduction rate of the subgrade and the grouting opportunity. With the extension of grouting opportunity and the decrease in OB/IB, the subsidence reduction ratio at the center of the subgrade decreases in an exponential curve.

In the simulation process of this article, the results of large-scale mining cases under real overburden were not verified, which requires further improvement based on the simulation in this article.

Author Contributions: Conceptualization, H.W. and Y.Q.; methodology, Y.Q. and Y.G.; software, H.W. and Y.G.; validation, Y.Q. and N.X.; formal analysis, Y.G. and Y.Q.; investigation, H.W. and Y.Q.; resources, Y.Q. and N.X.; data curation, Y.G. and Y.Q.; writing—original draft preparation, Y.G. and Y.Q.; writing—review and editing, Y.Q. and N.X.; visualization, H.W. and Y.G.; supervision, Y.Q. and N.X.; project administration, Y.Q.; funding acquisition, N.X. All authors have read and agreed to the published version of the manuscript.

Funding: This research was funded by National Natural Science Foundation of China (NSFC) under grant no. 42230709 with the title "Mechanism and prevention methods of tunnel disaster induced by long-term deformation of rock strata in mining-induced subsidence zone".

Data Availability Statement: Not applicable.

Acknowledgments: The authors thank the National Natural Science Foundation of China (NSFC) under Grant No. 42230709.

Conflicts of Interest: The authors declare no conflict of interest.

References

1. Wang, H.; Li, Y.; Dun, Z.; Cheng, J.; Dun, Z.; Wu, C. Seepage Grouting Mechanism for Foundations in Goaf Sites considering Diffusion Paths. *Geofluids* **2022**, *2022*, 8394811. [CrossRef]
2. Wei, X.; Bai, H.; Rong, H.; Jiao, Y.; Zhang, B. Research on Mining Fracture of Overburden in Close Distance Multi-seam. *Procedia Earth Planet. Sci.* **2011**, *2*, 20–27. [CrossRef]
3. Zhang, M.; Shimada, H.; Sasaoka, T.; Matsui, K.; Dou, L. Evolution and effect of the stress concentration and rock failure in the deep multi-seam coal mining. *Environ. Earth Sci.* **2013**, *72*, 629–643. [CrossRef]
4. Adhikary, D.; Khanal, M.; Jayasundara, C.; Balusu, R. Deficiencies in 2D Simulation: A Comparative Study of 2D Versus 3D Simulation of Multi-seam Longwall Mining. *Rock Mech. Rock Eng.* **2016**, *49*, 2181–2185. [CrossRef]

5. Ma, W.-M.; Zhu, W.-Y. Effect of multi-seam mining on subsidence. *Int. J. Min. Eng.* **1984**, *2*, 171–173. [CrossRef]
6. Ren, G.; Li, G.; Kulessa, M. Application of a Generalised Influence Function Method for Subsidence Prediction in Multi-seam Longwall Extraction. *Geotech. Geol. Eng.* **2014**, *32*, 1123–1131. [CrossRef]
7. Ma, W.J.; Hu, H.F. The Strata Movement Regularity and Parameter Simulation Analysis in Multiple Seams Repeated Mining. *Appl. Mech. Mater.* **2013**, *295–298*, 2935–2939. [CrossRef]
8. Ying-Ke, L.; Fu-Bao, Z.; Lang, L.; Chun, L.; Shen-Yong, H. An experimental and numerical investigation on the deformation of overlying coal seams above double-seam extraction for controlling coal mine methane emissions. *Int. J. Coal Geol.* **2011**, *87*, 139–149. [CrossRef]
9. Ghabraie, B.; Ren, G.; Smith, J.V. Characterising the multi-seam subsidence due to varying mining configuration, insights from physical modelling. *Int. J. Rock Mech. Min. Sci.* **2017**, *93*, 269–279. [CrossRef]
10. Ghabraie, B.; Ren, G.; Barbato, J.; Smith, J.V. A predictive methodology for multi-seam mining induced subsidence. *Int. J. Rock Mech. Min. Sci.* **2017**, *93*, 280–294. [CrossRef]
11. Salmi, E.F.; Nazem, M.; Deng, K.Z.; Karakus, M. Numerical analysis of a large landslide induced by coal mining subsidence. *Eng. Geol.* **2017**, *217*, 141–152. [CrossRef]
12. Bin Zhang, X. The Probe Technology and Counter Measures of Goaf of Colliery Area in Tongluoshan Tunnel. *Appl. Mech. Mater.* **2012**, *204–208*, 1419–1422. [CrossRef]
13. Zha, W.H. Reinforced Techniques Analysis of Goaf-Side Entry at Isolated Island Coal Face Based on FLAC Numerical Simulation. *Adv. Mater. Res.* **2012**, *605–607*, 210–214. [CrossRef]
14. Cai, W.; Chang, Z.; Zhang, D.; Wang, X.; Cao, W.; Zhou, Y. Roof filling control technology and application to mine roadway damage in small pit goaf. *Int. J. Min. Sci. Technol.* **2018**, *29*, 477–482. [CrossRef]
15. Xie, S.; Pan, H.; Zeng, J.; Wang, E.; Chen, D.; Zhang, T.; Peng, X.; Yang, J.; Chen, F.; Qiao, S. A case study on control technology of surrounding rock of a large section chamber under a 1200-m deep goaf in Xingdong coal mine, China. *Eng. Fail. Anal.* **2019**, *104*, 112–125. [CrossRef]
16. Bai, H.R.; Li, J.J. Evaluation of Grouting Effect Detection in Goaf. *Appl. Mech. Mater.* **2013**, *438–439*, 1080–1083. [CrossRef]
17. Ao, X.; Wang, X.; Zhu, X.; Zhou, Z.; Zhang, X. Grouting Simulation and Stability Analysis of Coal Mine Goaf Considering Hydromechanical Coupling. *J. Comput. Civ. Eng.* **2017**, *31*, 04016069. [CrossRef]
18. Wu, X.; Wang, S.; Tian, C.; Ji, C.; Wang, J. Failure Mechanism and Stability Control of Surrounding Rock of Docking Roadway under Multiple Dynamic Pressures in Extrathick Coal Seam. *Geofluids* **2020**, *2020*, 8871925. [CrossRef]
19. Li, X.; Guo, X.; Sun, G. Grouting Reinforcement Mechanism and Multimodel Simulation Analysis of Longwall Goaf. *Geofluids* **2021**, *2021*, 13. [CrossRef]
20. Hu, Z.; Ma, B.; Chen, X.; Chen, L. Study on Sensitivity Parameters Analysis of Grouting Reinforcement Underpassing Existing Subway Tunnel by Numerical Modeling. *Adv. Civ. Eng.* **2021**, *2021*, 13. [CrossRef]
21. Xuan, D.; Li, J.; Zheng, K.; Xu, J. Experimental Study of Slurry Flow in Mining-Induced Fractures during Longwall Overburden Grout Injection. *Geofluids* **2020**, *2020*, 8877616. [CrossRef]
22. Yu, W.; Li, K.; Liu, Z.; An, B.; Wang, P.; Wu, H. Mechanical characteristics and deformation control of surrounding rock in weakly cemented siltstone. *Environ. Earth Sci.* **2021**, *80*, 337. [CrossRef]
23. Liu, B.; Sang, H.; Wang, Z.; Kang, Y. Experimental Study on the Mechanical Properties of Rock Fracture after Grouting Reinforcement. *Energies* **2020**, *13*, 4814. [CrossRef]
24. Xie, S.; Wu, X.; Chen, D.; Sun, Y.; Wang, E.; Wu, X.; Duan, X.; Jiang, Z.; Qi, P.; Shi, S. Failure Mechanism and Control Technology of Thick and Soft Coal Fully Mechanized Caving Roadway under Double Gobs in Close Coal Seams. *Shock. Vib.* **2020**, *2020*, 8846014. [CrossRef]
25. Han, L.J.; He, Y.N. Experimental Study on Mechanical Characteristics of Cracked Rock Mass Reinforced by Bolting and Grouting. *J. China Univ. Min. Technol.* **2005**, *34*, 418–422.
26. Modoni, G.; Bzówka, J. Analysis of Foundations Reinforced with Jet Grouting. *J. Geotech. Geoenvironment. Eng.* **2012**, *138*, 1442–1454. [CrossRef]
27. Zong, Y.; Han, L.; Qu, T.; Yang, S. Mechanical properties and failure characteristics of fractured sandstone with grouting and anchorage. *Int. J. Min. Sci. Technol.* **2014**, *24*, 165–170. [CrossRef]
28. Wang, C.; Xiong, Z.; Wang, C.; Wang, Y.; Zhang, Y. Study on Rib Sloughage Prevention Based on Geological Structure Exploration and Deep Borehole Grouting in Front Abutment Zones. *Geofluids* **2020**, *2020*, 7961032. [CrossRef]
29. Deng, K.Z.; Tan, Z.X.; Zhang, H.Z. Design Method of Strip Grouting for Old Longwall Mining Goaf. *J. China Coal Soc.* **2008**, *161*, 153–156.
30. Chen, S.J.; Zhang, L.B.; Jiang, N.; Yin, D.; Gao, Z.; Guo, W. A case of large buildings construction above oldmine goaf in Shandong Province. *J. China Coal. Soc.* **2022**, *47*, 1017–1030.
31. He, F.; Lv, K.; Li, X.; Qin, B.; Li, L. Failure Mechanism and Control of Lower Retracement Channel in Close-Distance Double-Thick Coal Seams. *Shock. Vib.* **2021**, *2021*, 6651099. [CrossRef]

32. Shanxi Traff Layout Reconnaissance Design Inst Co. JTG/T D31-03. *Guidelines for Design and Construction of Highway Engineering in the Mined-Out Area*; People's Communications Publishing House: Beijing, China, 2011.
33. Qin, Y. *Restudy on Complex Mechanical Behavior of Rock Mass in Multi-Seam Mining*; China University of Geosciences: Beijing, China, 2021.
34. Yue, Z. *Simulation Study on Long-Term Deformation Law of Coal Mine Goaf Based on FLAC3D*; China University of Geosciences: Beijing, China, 2023.

Disclaimer/Publisher's Note: The statements, opinions and data contained in all publications are solely those of the individual author(s) and contributor(s) and not of MDPI and/or the editor(s). MDPI and/or the editor(s) disclaim responsibility for any injury to people or property resulting from any ideas, methods, instructions or products referred to in the content.